Saccadic adaptation to a systematically varying disturbance

Carlos R. Cassanello, Sven Ohl and Martin Rolfs

You might find this additional info useful...

This article cites 80 articles, 36 of which you can access for free at:
http://jn.physiology.org/content/116/2/336.full#ref-list-1

Updated information and services including high resolution figures, can be found at:
http://jn.physiology.org/content/116/2/336.full

Additional material and information about *Journal of Neurophysiology* can be found at:
http://www.the-aps.org/publications/jn

This information is current as of August 10, 2016.

Saccadic adaptation to a systematically varying disturbance

Carlos R. Cassanello, Sven Ohl, and Martin Rolfs

Department of Psychology and Bernstein Center for Computational Neuroscience, Humboldt Universität zu Berlin, Berlin, Germany

Cassanello CR, Ohl S, Rolfs M. Saccadic adaptation to a systematically varying disturbance. *J Neurophysiol* 116: 336–350, 2016. First published April 20, 2016; doi:10.1152/jn.00206.2016.—Saccadic adaptation maintains the correct mapping between eye movements and their targets, yet the dynamics of saccadic gain changes in the presence of systematically varying disturbances has not been extensively studied. Here we assessed changes in the gain of saccade amplitudes induced by continuous and periodic postsaccadic visual feedback. Observers made saccades following a sequence of target steps either along the horizontal meridian (Two-way adaptation) or with unconstrained saccade directions (Global adaptation). An intrasaccadic step—following a sinusoidal variation as a function of the trial number (with 3 different frequencies tested in separate blocks)—consistently displaced the target along its vector. The oculomotor system responded to the resulting feedback error by modifying saccade amplitudes in a periodic fashion with similar frequency of variation but lagging the disturbance by a few tens of trials. This periodic response was superimposed on a drift toward stronger hypometria with similar asymptotes and decay rates across stimulus conditions. The magnitude of the periodic response decreased with increasing frequency and was smaller and more delayed for Global than Two-way adaptation. These results suggest that—in addition to the well-characterized return-to-baseline response observed in protocols using constant visual feedback—the oculomotor system attempts to minimize the feedback error by integrating its variation across trials. This process resembles a convolution with an internal response function, whose structure would be determined by coefficients of the learning model. Our protocol reveals this fast learning process in single short experimental sessions, qualifying it for the study of sensorimotor learning in health and disease.

visually guided saccades; sensorimotor learning; oculomotor plasticity; parameter estimation; delta rule; state equation; response function

NEW & NOTEWORTHY

Saccadic adaptation maintains the mapping between rapid eye movements and their visual targets. We studied the dynamics of this process, using an intrasaccadic target displacement that changed in size as a sinusoidal function of the trial number. The oculomotor response displayed two independent components—a delayed periodic change in saccade gain superimposed on a drift toward higher hypometria (despite the displacements' zero mean). We quantified this response and discuss possible origins and underlying learning processes.

OCULAR SACCADES are fast and accurate eye movements that rapidly recenter gaze to sample relevant information in the

visual environment. Because of their ballistic nature, they need to be preprogrammed and online visual feedback cannot be used to correct the ongoing movement. Mechanisms of saccadic adaptation therefore must largely rely on past experience and active predictions (Chen-Harris et al. 2008; Ethier et al. 2008a) rather than closed-loop sensory information to maintain the accuracy of saccades by adjusting the amplitude (Herman et al. 2013; Hopp and Fuchs 2004; McLaughlin 1967) or direction (Azadi and Harwood 2014; Collins et al. 2010; Harwood and Wallman 2004) of subsequent movements.

Adaptation in saccade amplitude can be revealed in the laboratory with a double-step protocol. The first step turns the (presaccadic) target into the goal or proxy for the upcoming saccade. The second step then systematically shifts the target to a position different from the saccade proxy, contingent with the onset of the eye movement and thus during the interval of suppression of displacement (Bridgeman et al. 1975). In most studies, this imperceptible intrasaccadic step (ISS) displaces the target by a constant proportion of the size of the first step in the direction along the target vector (Fig. 1*A*; McLaughlin 1967; for review see Hopp and Fuchs 2004). Substantial adaptation can be induced, even for ISS as small as 2.5% of the first step amplitude (Herman et al. 2013). At the beginning of a block of adapting trials, the constant ISS produces a commensurate postsaccadic visual error (VE) that decreases in size across trials as the oculomotor system progressively adjusts the amplitude of the saccade. Therefore, this protocol naturally features a passive systematic variation of the VE even when the inducing disturbance is apparently constant. Reciprocally, it is possible to keep the VE constant a posteriori of the saccade landing (Robinson et al. 2003; Fig. 1*B*), in which case the ISS will evolve temporally although still in a passive way. Note that in both cases a feature pertaining to the disturbance that was experimentally implemented to be constant inherited dynamics as a consequence of the error correcting process.

In the present study, we investigated how adaptation manifests in the presence of a disturbance that follows a continuous evolution on its own. Our objectives can be summarized as follows. First, we assessed whether the oculomotor system indeed showed a discernible and reproducible response that had structural features related to the disturbance. In fact, the system may respond in an unspecific way (e.g., Wei et al. 2010), for example, fluctuating around the mean of the surreptitious target displacement generated by the disturbance. Second, in parameterizing and fitting the observed response—that, as we show, was related to the disturbance—we sought a sensitive and reliable estimation procedure to obtain its parameters without requiring several repetitions of the experimental runs. Seeking these features in the experimental design would allow use of the protocol to study oculomotor plasticity in

Address for reprint requests and other correspondence: C. R. Cassanello, Dept. of Psychology and Bernstein Center for Computational Neuroscience, Humboldt Universität zu Berlin, Philippstr. 13 Haus 6, 10115 Berlin, Germany (e-mail: carlos.cassanello@bccn-berlin.de).
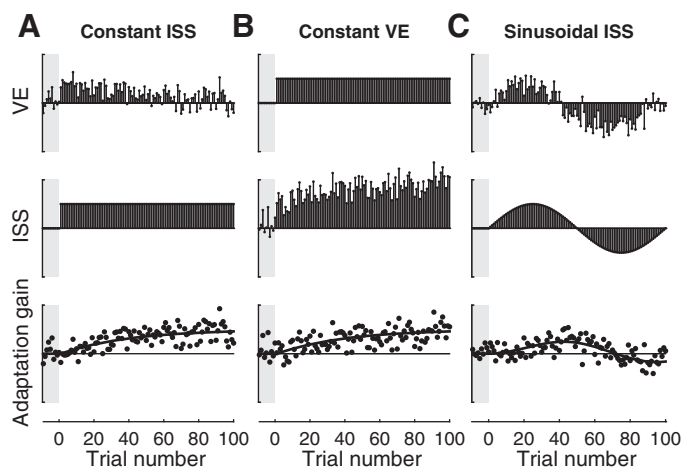
Fig. 1. Schematic of adaptation gain, intrasaccadic step, (ISS), and visual error (VE) over the course of preadaptation (gray shaded) and adaptation trials in double-step protocols used to study saccadic adaptation. *A*: fixed-ISS protocol: the magnitude of the second step (ISS) is a fixed proportion of the first (presaccadic) target step, administered contingent on saccade onset. *B*: fixed-VE protocol: the second step is also a fixed proportion of the first target step but applied to the eyes' landing position, contingent on saccade landing, resulting in a fixed VE. *C*: sinusoidal ISS protocol used in this study: the ISS magnitude changes trial by trial, following a sinusoidal dependence on the trial number.

clinical populations of patients with focal cerebellar and thalamo-cortical lesions (e.g., Alahyane et al. 2008b; Ostendorf et al. 2010, 2012; Panouillères et al. 2013) and patients with various neurological or mental disorders (e.g., Golla et al. 2007; Rösler et al. 2015; review in MacAskill et al. 2002) as well as in aging groups (e.g., Bock et al. 2014). Third, we were curious to investigate whether the learning process induced by a disturbance endowed with a temporally structured variation would unveil new features that were not accessible with the fixed-step protocol. These features could further constrain current models of sensorimotor learning, for example, with respect to the number and dynamics of the learning processes involved, the nature of the biases encountered, the window of integration that the system needs to track to mitigate the features of the disturbance, as well as possible dissociations between oculomotor bias and error correction-based effects.

To fulfill these goals we adapted a protocol recently introduced in a study of manual reach movements (Hudson and Landy 2012) to study changes in saccadic amplitude under a gradually and periodically changing but otherwise noise-free stimulus (Fig. 1*C*).[1] Observers made saccades to targets that underwent an ISS with sinusoidal variation across trials. Across experimental sessions, we manipulated the frequencies of these sinusoidal variations within the same subjects. For two different types of adaptation, Two-way and Global (Garaas and Pomplun 2011; Rolfs et al. 2010), the oculomotor system responded to these surreptitious sinusoidal target displacements by acquiring a sinusoidal variation of commensurate frequency in the amplitude of the saccades that lagged the ISS by a few tens of trials. This periodic response was superimposed on a drift of the baseline of the saccade landing, which in almost all cases monotonically increased the participant's hypometria. On the basis of these findings, we discuss how our

[1] A reviewer pointed out to us a related experimental protocol, presented at the Society for Neuroscience Meeting in 2004 (Harwood and Wallman 2004).

paradigm may help unveil modifications needed to constrain or revise models of error-correcting mechanisms and make them consistent with the rich dynamics of plasticity in saccadic behavior. In particular, we argue that both components of the oculomotor response can be captured qualitatively with a simple learning algorithm known as the delta rule (Baddeley et al. 2003; Nassar et al. 2010; Rescorla and Wagner 1972; Srimal et al. 2008; Sutton and Barto 1981)—or a variant of it—in which the amplitude of the upcoming saccade results from weighting the predicted size of the last saccade (possibly with imperfect retention; e.g., Rolfs et al. 2010; Smith et al. 2006) and the last experienced VE. Because, in our paradigm the disturbance possesses dynamics of its own (as opposed to fixed-step protocols), the iteration implicit in the delta rule dissociates the effects produced by the constant components of the disturbance from those associated with its trial-by-trial variation. Thus the oculomotor response would arise from a process that resembles a response function that weights and integrates the disturbance experienced over some temporal window. In this framework, we argue, the lag and amplitude of the periodic component, and the asymptotic value of the baseline drift in the experimentally observed oculomotor response, may help determine the size of the learning parameters as well as the extent of the window of integration.

MATERIALS AND METHODS

Participants

Ten observers (age 20–55 yr, 5 women, 5 men; 7 right eye dominant, all right-handed) with normal or corrected-to-normal vision performed the experiment. Two authors participated; all remaining participants were naive with respect to the purposes of the experiment. The experimental protocols were submitted to and approved by the Institutional Review Board of the Psychology Department of the Humboldt University of Berlin. We obtained written informed consent from all participants prior to their inclusion in the study, which conformed to the Declaration of Helsinki.

Setup

Participants sat in a darkened room with their head stabilized with chin and forehead rests, 57 cm from a Sony GDM-FW900 24-in. CRT screen (1,280 × 800 pixels, 100-Hz vertical refresh rate). We recorded movements of the dominant eye (determined for each observer with a hole-in-card test) with an EyeLink 1000 system (SR Research, Osgoode, ON, Canada) having an average spatial resolution of 15–30 min-arc of visual angle and a sampling rate of 1,000 Hz. The experiment was controlled with the Psychophysics (Brainard 1997; Kleiner et al. 2007; Pelli 1997) and EyeLink (Cornelissen et al. 2002) toolboxes for MATLAB (MathWorks, Natick, MA).

Procedure

We tested each observer in two different protocols (Fig. 2, *A–D*): Whereas Two-way adaptation yields vector-specific adaptation fields (e.g., Alahyane et al. 2008a; Albano 1996), Global adaptation results in a change in saccade gain that affects all saccade vectors (Garaas and Pomplun 2011; Rolfs et al. 2010). We ran each protocol in separate sessions, with at least 1 day in between, and counterbalanced their order across observers. Each session started with a standard nine-point grid calibration-validation procedure of the eye tracker, which we repeated whenever fixation could no longer be detected in a circular fixation area with a radius of 1.5 degrees of visual angle (dva) centered on the target (Fig. 2, *C* and *D*). Each of the two sessions
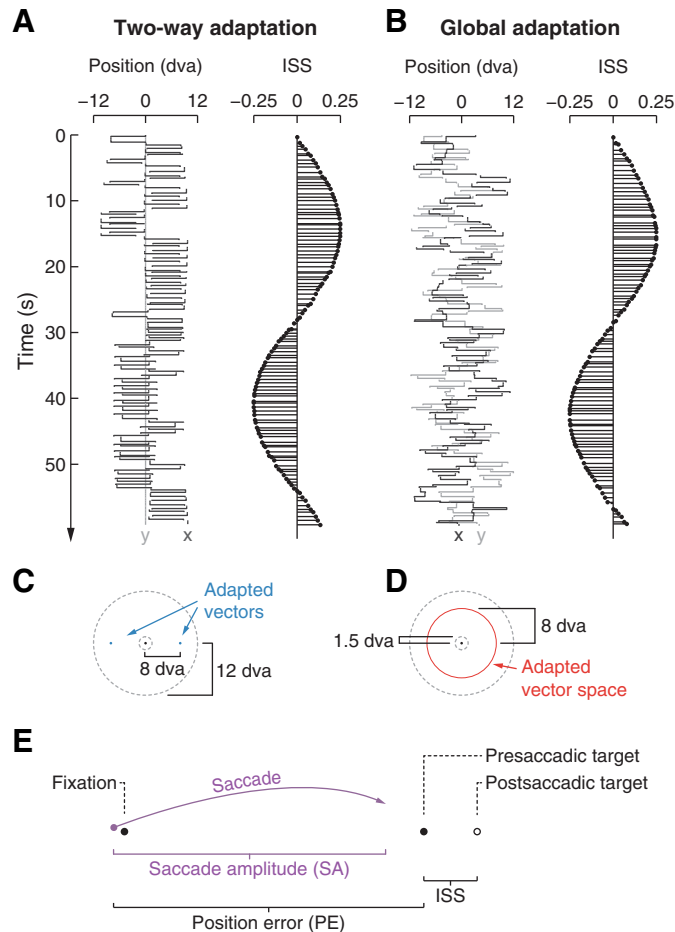
Fig. 2. Adaptation protocols and definition of variables. *A*: Two-way adaptation with 100 trials per cycle (6 cpb condition). On each trial, the fixation target was displaced horizontally with fixed amplitude of 8 dva, starting at the center of the screen (*left*). The ISS of the fixation target followed a sinusoidal modulation with an amplitude of 0.25 of the presaccadic target displacement (*right*). Note that fixation on each trial started at the last position of the target on the previous trial. *B*: Global adaptation with 100 trials per cycle (6 cpb condition). On each trial, the fixation target was displaced in a random direction with fixed amplitude of 8 dva, starting at the center of the screen (*left*). The ISS of the fixation target followed a sinusoidal modulation with amplitude of 0.25 of the presaccadic target displacement in the radial direction along the presaccadic target vector (*right*). *C* and *D*: adapted saccade vectors, fixation, and target areas (dotted lines) in the Two-way and Global conditions, respectively, drawn to scale. *E*: schematic of the experimental variables used to calculate adaptation gain.

lasted ~50 min, during which observers performed a total of 2,200 trials distributed across seven blocks. We obtained this large number of trials by using a fast-paced protocol, which uses reduced fixation periods between consecutive trials to induce efficient saccadic adaptation (Gray et al. 2014). *Blocks 1*, *3*, *5*, and *7* had 100 trials each with no ISS. *Blocks 2*, *4*, and *6* were adaptation blocks and contained 600 trials in which the ISS was varied in a sinusoidal fashion between −25% and +25% of the amplitude of the presaccadic target displacement. The three adaptation blocks (conditions) differed in the number of cycles in the corresponding 600-saccade adaptation block. In the 3, 4, and 6 cycles per block (cpb) conditions, it took 200, 150, and 100 trials to complete a full cycle, respectively, which in turn represented 0.5, 0.67, and 1 ISS cycle per 100 trials. The order of these blocks was randomly chosen for each observer and session. The program was paused after each adaptation block, giving participants some resting time. We calibrated eye position routinely at the beginning of each nonadapting block. Because of the rather precise timing characteris-

tics of saccade adaptation in our protocols, recalibration introduces a fairly harmful perturbation. We minimized the necessity of recalibration in adaptation blocks by advising observers at the beginning of the experiment to maintain their head as steady as possible. Additional recalibration of the eye tracker during the experiment was necessary only in rare, isolated cases.

A trial started with presentation of a red fixation point, 0.3 dva in diameter, against a gray background. When the position of the dominant eye was detected within the fixation area of 1.5 dva from that fixation point for at least 200 ms, the fixation point turned black and, after a fixation period of 50–350 ms (drawn from a uniform distribution), it was displaced to a new position to become the target for the impending saccade, with the constraint that the target remained within the invisible borders of a circular target area (radius of 12 dva, centered on the screen; Fig. 2, *C* and *D*). We instructed participants to move their eyes quickly to this newly defined saccade target.

The first trial started from the screen center, and subsequent trials continued from the latest target position. We ensured that observers followed the target with the eyes by monitoring gaze position throughout the trial. After target onset, saccades were detected online as soon as the gaze left the boundary of a circular fixation area (1.5 dva around the fixation point). In adapting trials, saccades triggered an ISS of the target stimulus (see below), displacing it along the direction of the saccade in the next screen refresh. On each trial of Two-way adaptation, the fixation target stepped horizontally to a presaccadic target location at 8 dva eccentricity, either to the left or to the right of the fixation point (Fig. 2, *A* and *C*). On each trial of Global adaptation, the fixation target stepped in a random direction (0–359° polar angle, in steps of 1° polar angle) to a presaccadic target location at 8 dva eccentricity (Fig. 2, *B* and *D*). The target was almost always (99.96% of all trials) displaced before the eye landed (median of 30 ms before saccade offset) and invariably within one screen refresh of saccade landing, during saccadic suppression of displacement (Bridgeman et al. 1975). The next trial started 200 ms after saccade onset. If fixation broke because of blinks or large eye movements during the fixation period, a warning appeared on the screen asking observers to maintain fixation and the trial was rerun immediately.

Data Analysis

Saccade detection and trial exclusion. For data analysis, we detected saccades off-line with an algorithm by Engbert and Mergenthaler (2006). Saccades were detected as outliers in the distribution of 2D velocities of each trial (smoothed over 5 subsequent eye position samples), exceeding the median velocity by 5 SD for at least 8 ms. Events separated by ≤20 ms were merged into a single saccade, as overshoots in saccades often result in the detection of two saccades. Response saccades were defined as the first saccade that brought the eye into a circular region around the presaccadic target with a radius of half its eccentricity (4 dva). We excluded 3.42% (1,232 of 36,000) of all trials from further analyses because blinks, the absence of a response saccade, or saccades > 1 dva before a response saccade were detected.

Modeling of the saccadic response. The target ISS followed a sinusoidal change across trials:

$$\text{ISS} = P \cdot \sin\left(\frac{2\pi f}{N} n\right) \tag{1}$$

Here, *f* is the frequency of the sinusoid in cycles per block, *N* is the number of trials in an adaptation block, and *n* is the index of the current trial. *P* is the maximum absolute magnitude of the ISS, i.e., the amplitude of the sinusoid that defines the ISS. It was fixed at 2 dva, so that the ISS changed in magnitude periodically and in a sinusoidal fashion between −25% and +25% of the magnitude of the presaccadic target eccentricity (8 dva). At fixed amplitude, the ISS at trial *n* is fully determined by the angular frequency $2\pi f/N$ that

characterizes the rate of change of the sinusoid in each trial. Given that we used a fixed number of trials per adaptation block and a single ISS amplitude ($P = 2$ dva), throughout this article we express magnitude values as fractions of P and the frequency as the number of cycles per block (cpb). In all experiments, we set the initial phase to 0, which means that the magnitude of the ISS starts at 0 in the direction of positive ISS (outward steps of the saccade target) first.

Saccadic amplitude adaptation is usually described in terms of the changes in saccade gain (SG), defined as the ratio of the saccade amplitude (SA) to the presaccadic position error (PE; Fig. 2E). During nonadapting trials and at the beginning of the adaptation blocks, SG is typically slightly smaller than 1, which means that the saccade undershoots the target. Here, we were primarily concerned with how closely the changes in SA resembled the disturbance. Thus we considered the changes of the adaptation gain, defined as the landing error, SA $-$ PE, expressed as a proportion of P, the constant amplitude of the ISS:

$$\text{adaptation gain} \cong \frac{\text{SA} - \text{PE}}{P} = \left(\frac{\text{SA}}{\text{PE}} - 1\right) \cdot \frac{\text{PE}}{P} = (\text{SG} - 1) \cdot \frac{\text{PE}}{P} \quad (2)$$

Note that PE is measured from the eye position at saccade onset (not necessarily coincidental with the position of the fixation point; Fig. 2E). This definition of saccade landing error was easy to generalize to the random direction geometry used in the Global adaptation condition. *Equation 2* also gives a correspondence between our definition of adaptation gain and the usual saccade gain, SG = SA/PE. Clearly, when SG equals 1, adaptation gain vanishes. Our definition therefore adopts the nonadaptation situation as the zero reference point. The presence of hypometria then manifests as a slightly negative baseline in the adaptation gain. As adaptation kicks in, *Eq. 2* quantifies the departure of SG from 1 magnified by the ratio PE/P (i.e., ~8/2 = 4 in our experiments).

To obtain an idea of general patterns present in the data we first alleviated baseline differences between participants. To this end, we removed the mean from the adaptation gain of each adaptation block for each participant. Then we collapsed across participants the data for each frequency and each adaptation type tested and fitted a number of functional dependences to the resulting mean using MATLAB's nlinfit. A model comparison using the Akaike information criterion (AIC; Akaike 1974, 1978) and the Bayesian information criterion (BIC; Schwarz 1978; for comparison of the criteria and the specific definitions used see Bozdogan 1987; Wang and Liu 2006) suggested that the functional form

$$\text{adaptation gain} \cong \frac{\text{SA} - \text{PE}}{P} = B \cdot \exp(-\alpha \cdot n) + B_\text{o} +$$
$$A \cdot \sin\left(\frac{2\pi\nu}{N}n - \phi\right) \quad (3)$$

is the best-fitting model to the averages of the demeaned data across participants in all conditions tested (see comparison to alternative models in Table 2 in *Average Oculomotor Response and Model Selection*). This model consists of a drift that is described as an exponential decay to some baseline asymptote B_o, with amplitude B and a timescale given by α^{-1}. In addition, we hypothesized that the oculomtor response followed a periodic change similar to that present in the ISS (see also Hudson and Landy 2012), where A was the maximum absolute magnitude (amplitude), ν was the frequency, and ϕ described the lag of the oculomotor response with respect to the ISS. The frequency ν might or might not match the frequency of the disturbance, f, and the lag ϕ could be expressed as a phase in the sinusoid or as a number of trials n_0, using the identity $\phi = (2\pi\nu/N)n_0$.

Parameter estimation. To estimate parameters of a putative underlying distribution that is most likely to have generated the values of

the data set collected, we used a Gaussian likelihood function. We assumed that the data collected from each participant could be predicted by *Eq. 3* (with the individual mean restored) up to an additive error (noise) that was normally distributed with a standard deviation of σ, so that the data recorded in trial n were assumed to be given by $d(n) =$ adaptation gain $+ \varepsilon(n)$ and the likelihood of the data given the model became

$$\Pi_{n=1}^{N} \frac{1}{\sqrt{2\pi\sigma^2}} \cdot \exp\left(-\frac{\varepsilon(n)^2}{2\sigma^2}\right)$$
$$= (2\pi\sigma^2)^{-\frac{N}{2}} \cdot \exp\left\{-\frac{1}{2\sigma^2}\sum_{n=1}^{N}(d(n) - \text{adaptation gain})^2\right\} \quad (4)$$

Thus each specific model for the oculomotor response within the set explored was defined and indexed by a specific set of values of the parameters described in *Eq. 3*. The power of the noise representing the error, σ, was a nuisance parameter (in which we were not interested). From a Bayesian point of view, the effect of parameters irrelevant to the purposes of the study could be accounted for by integrating over all possible values they could take, weighted by an appropriate prior probability distribution reflecting all information about such parameters available beforehand. If little or no information were available about a parameter to be integrated, a common procedure is to use a noninformative prior based solely on the mathematical properties that a probability distribution must obey. In the case of the standard deviation of Gaussian noise, $1/\sigma$ is an appropriate noninformative prior (Bretthorst 1988; Hudson and Landy 2012; Jeffreys 1946; Kass and Raftery 1995). After integration over the noise parameter using the prior $1/\sigma$, the resulting joint probability density for the remaining parameters had the form

$$p(B, B_\text{o}, \alpha, A, \nu, \phi) \approx \left[\sum_{n=1}^{N}\left(B \cdot \exp(-\alpha \cdot n) + B_\text{o} + \right.\right.$$
$$\left.\left. A \cdot \sin\left(\frac{2\pi\nu}{N}n - \phi\right) - d(n)\right)^2\right]^{-\frac{N}{2}} \quad (5)$$

Finally, we obtained a posterior probability density for each parameter by integrating the joint density over the remaining parameters (for details, see Hudson and Landy 2012).

The estimation procedure we used required a choice of prior probabilities for each of the three parameters A, ν, and ϕ for the sinusoidal component and each of the three parameters for the drift in the baseline, B, B_o, and α. We chose uniform priors for all nonnuisance parameters. For the frequency, we selected a range between 2 and 8 cpb, including all ISS frequencies tested (3, 4, and 6 cpb). For the amplitude, informed by the data we limited the range to 0.3 since the amplitude of the sinusoidal component of the adaptation gain rarely reached 25% of the ISS amplitude. The lag was a circular variable because it was associated with a phase of a sinusoidal function. Therefore, we limited the prior distribution to one complete cycle to avoid the appearance of double peaks.

After a first estimation of all parameters we inspected the posterior distributions for the frequency because, as pointed out above, this was the only parameter determining the dynamics of the disturbance. We identified the mode of the posterior distributions for the frequency and corroborated that they matched well those of the disturbance (see *Validation of Parameter Estimation Procedure*; Fig. 5, *E* and *F*). Because uncertainty in the frequency affects the width in the posterior distribution of the lag parameter and possibly that of the amplitude, and because the data showed a coexistent (exponential) drift in the baseline involving the estimation of three other parameters, we decided to conduct the estimation in a hierarchical sequence. Therefore, we used a Dirac's δ-function centered on this estimate as a prior for the frequency and reestimated posterior distributions for all other parameters.

Statistics. Throughout this article we report results as means ± SD for individual data and means ± SE when we discuss recordings or estimates across participants. To determine average parameters from the parameter estimation other than the frequency, we computed the mean and variance for each parameter and participant as the first two moments of the corresponding posterior probability distribution and took the average of the means weighted by their SDs (square root of the estimated variance) to generate each point on the population plot (see Fig. 6, *A–F, right*). Alternative estimators (e.g., the modes of the posterior densities, with and without weighting) gave qualitatively similar results.

We used 2 × 3 repeated-measures ANOVAs to assess the influence of the type of adaptation (Two-way vs. Global) and ISS frequency (3 vs. 4 vs. 6 cpb) on any dependent variable. To preempt potential violations of the sphericity assumption of the ANOVA, we applied Greenhouse-Geisser correction to the degrees of freedom. To follow up on interactions between two factors, we conducted post hoc comparisons using *t*-tests and adjusted the α level for multiple comparisons with Bonferroni correction.

RESULTS

Overall Saccade Parameters

Mean saccade latency and duration were similar across adaptation and nonadaptation blocks and across all three frequencies tested (Table 1). Saccade latency was slightly lower in the Two-way (156 ± 7 ms) than the Global (164 ± 6 ms) adaptation session, as evidenced in a main effect of adaptation type [$F_{(1,9)} = 6.90$, $P = 0.027$]. Reduced latencies for Two-way adaptation were likely a consequence of the much higher predictability of target location (e.g., Rolfs and Vitu 2007). ISS frequency had no influence on saccade latency, and there was no interaction with adaptation type (all $F < 1$).

Saccade amplitudes were mostly hypometric (Table 1), with means over blocks and participants ranging from 68% to 101% of the presaccadic target amplitude (8 dva). They did not significantly differ between Global and Two-way adaptation blocks [$F_{(1,9)} = 2.81$, $P = 0.128$]. ISS frequency also had no influence on SA [$F_{(1.23,11.09)} = 1.14$, $P > 0.250$], and there was no interaction with adaptation type [$F_{(1.88,16.90)} < 1$]. However, comparing mean values of the saccade amplitude, hypometria appeared more pronounced during adapting compared with nonadapting trials both during Two-way adaptation (7.27 ± 0.13 vs. 7.49 ± 0.12 dva) and during Global adaptation (7.04 ± 0.17 vs. 7.22 ± 0.15 dva), suggesting that adaptation trials enhance the tendency to undershoot [$t_{(9)} = 6.01$, $P < 0.001$].

Saccade duration was independent of adaptation type [$F_{(1.23,11.09)} = 1.14$, $P > 0.250$], ISS frequency, or their interaction (all $F < 1$). Similarly, the mean peak velocity did not significantly vary with any experimental condition (all $F < 1$).

Average Oculomotor Response and Model Selection

To obtain an idea of general patterns present in the data, we first alleviated baseline differences between participants. To this end, we removed the mean from the adaptation gain of each adaptation block for each participant. Then we collapsed across participants the data for each frequency and each adaptation type tested. We fitted a number of functional dependences to the resulting mean across participants using MATLAB's nonlinear regression functions nlinfit (to obtain parameters that provide the best fit) and nlparci (to obtain 95% confidence intervals of the best-fitting parameters). After a formal model comparison using AIC and BIC, we selected model B+D+S from those listed in Table 2. The mean of the block across participants was then reinstated to overlap the fits with the data (Fig. 3). Model B+D+S was then implemented for the individual Bayesian estimation with the corresponding mean included (cf. *Eq. 3*). The best-fitting model included not only the sinusoidal variation but also a drift in the baseline that has been fitted with an exponential decay. Note that models that included slight modulation of the amplitude of the sinusoidal component were also competitive (not shown). However, those models were competitive only in the (noisier) Global adaptation data and required an extra parameter, and the timescale fitted was significantly larger than the timescale fitted to the baseline drift. Therefore, on the basis of parsimony and simplicity we adopted the model with fewer parameters that avails easier interpretation and suffices to account for the data presented here.

Analysis of Saccadic Response at Individual Level

First, we present the analysis of the saccadic response to the sinusoidal ISS for an example of a single participant (*observer IW*) who is representative of the entire sample. During Two-way adaptation (Fig. 4A; 3 cpb ISS frequency), the adaptation gain revealed a slow periodic modulation as a function of trial number, which is captured by the parametric fit of the saccadic response to the ISS.

Using the hierarchical parameter estimation procedure (see MATERIALS AND METHODS), we identified the mode of the posterior distribution for the frequency (Fig. 4B). We then used a Dirac's δ-function centered on this estimate as a prior for the frequency and reestimated posterior distributions for the amplitude and lag parameters, as well as the parameters

Table 1. *Saccade parameters segregated by block and type of adaptation*

	Condition	Preceding Nonadapting	3 cpb Adapting	Preceding Nonadapting	4 cpb Adapting	Preceding Nonadapting	6 cpb Adapting	Last Nonadapting
Latency, ms	Two-way	150 ± 7	156 ± 7	156 ± 7	155 ± 6	150 ± 8	156 ± 8	156 ± 8
	Global	161 ± 6	164 ± 6	161 ± 6	164 ± 6	163 ± 6	163 ± 6	161 ± 5
Amplitude, dva	Two-way	7.61 ± 0.14	7.29 ± 0.16	7.54 ± 0.16	7.26 ± 0.12	7.52 ± 0.11	7.28 ± 0.14	7.28 ± 0.15
	Global	7.33 ± 0.16	7.11 ± 0.15	7.21 ± 0.13	6.98 ± 0.14	7.31 ± 0.18	7.04 ± 0.21	7.04 ± 0.19
Duration, ms	Two-way	47 ± 3	49 ± 3	47 ± 3	49 ± 3	48 ± 3	49 ± 3	47 ± 3
	Global	46 ± 4	47 ± 4	44 ± 4	46 ± 4	44 ± 4	46 ± 4	44 ± 4
Peak velocity, dva/s	Two-way	418 ± 23	432 ± 24	411 ± 21	420 ± 22	419 ± 26	433 ± 25	411 ± 21
	Global	446 ± 34	453 ± 31	423 ± 32	444 ± 37	427 ± 33	453 ± 39	420 ± 33

Values are means ± SE across 10 participants for saccade parameters segregated by block and type of adaptation (Global vs. Two-way). Nonadapting blocks (zero ISS) had 100 trials; adapting blocks had 600 trials with ISS having cycles of 200, 150, and 100 saccades that resulted in a total of 3, 4, or 6 cpb. Adaptation blocks occurred in a random order during each session but were sorted here to show the data ordered by experimental condition.

Table 2. *Model comparison across five different models of the oculomotor response in the Two-way and Global adaptation conditions*

Model	Equation	#	MSE Two-way 3	4	6	MSE Global 3	4	6	AIC (BIC) Two-way 3	4	6	AIC (BIC) Global 3	4	6
B+D+S	$b_1 \cdot \sin\left(\dfrac{2\pi}{N} b_2(n - b_3)\right) + b_4 \cdot \exp(-b_5 n) + b_6$	6	0.0140	0.0138	0.0122	0.0256	0.0203	0.0219	0 (0)	0 (0)	0 (0)	0 (0)	0 (0)	0 (0)
S/BS	$b_1 \cdot \sin\left(\dfrac{2\pi}{N} b_2(n - b_3)\right) + b_4$	3	0.0194	0.0184	0.0163	0.0290	0.0217	0.0245	187 (174)	169 (156)	167 (154)	68 (54)	34 (20)	61 (48)
B+D	$b_1 \cdot \exp(-b_2 n) + b_3$	3	0.0281	0.0246	0.0200	0.0297	0.0240	0.0235	409 (396)	343 (330)	292 (279)	82 (68)	94 (81)	38 (25)
D	$b_1 \cdot \exp(-b_2 n)$	2	0.0321	0.0270	0.0212	0.0319	0.0246	0.0244	487 (469)	395 (377)	323 (305)	124 (106)	106 (89)	57 (40)
B	$b_1 = 0$	—*	0.0352	0.0296	0.0244	0.0325	0.0246	0.0250	540 (513)	448 (421)	405 (379)	129 (103)	103 (76)	67 (41)

Models consist of baseline (B), drift (D), and/or sinusoidal (S) components and have variable numbers of free parameters (#). MSE, mean squared error of the fitting to the demeaned data; AIC, Akaike information criterion; BIC, Bayesian information criterion. *In this model, was simply set to the mean of the (demeaned) data, that is, 0.

describing the baseline drift (Fig. 4*B*). The frequencies of the ISS used in each of the three conditions clearly reflect in the adaptation gain. For this observer, the estimated number of cycles of the gain for the three conditions tested—taken as the mode of the posterior distribution for the frequency parameter in the initial estimation—were $3 \pm 4e^{-03}$ cpb, 4 ± 0.04 cpb, and 6 ± 0.08 cpb, respectively (Fig. 4*B*, *top left*), corresponding almost exactly to 200, 150, and 100 saccades in each cycle for a total number of 600 trials in the block.

The amplitude of the adaptation gain (Fig. 4*B*, *top center*), expressed in units of the amplitude of the ISS (2 dva), can be taken as an indicator of how much of the ISS is reproduced by the adaptation. For this example observer, the estimated amplitudes of the adaptation gains were 0.23 ± 0.02, 0.17 ± 0.02, and 0.14 ± 0.02, corresponding to $23 \pm 2\%$, $17 \pm 2\%$, and $14 \pm 2\%$ of the amplitude of the ISS, respectively.

The estimated lags for the adaptation gain obtained from the corresponding posterior densities (Fig. 4*B*, *top right*) were 15.2 ± 2.6, 13.35 ± 2.4, and 8.5 ± 2.4 trials. Thus, with a small dependence on the frequency, the saccadic system adapted to the disturbance with a delay ranging between 8 and 15 trials.

The sinusoidal oculomotor response rides on a monotonic drift in adaptation gain, captured by an additional set of three parameters (Fig. 4*B*, *bottom*) defining an exponential function. For this observer, for the three successive frequency conditions of the Two-way adaptation type, the estimated values for B_o in *Eq. 3* were -0.68 ± 0.05, -0.70 ± 0.02, and -0.67 ± 0.07 of the ISS amplitude. The amplitude of the decay B was estimated to be 0.30 ± 0.06, 0.21 ± 0.05, and 0.50 ± 0.06 in the same units. Finally, α, the timescale of the exponential drift, was estimated to be $9e^{-03} \pm 7e^{-03}$, $8e^{-03} \pm 3e^{-03}$, and $7e^{-03} \pm 3e^{-03}$ trials^{-1}.

Adaptation gain in the Global adaptation condition (Fig. 4*C*; 3 cpb ISS frequency) also revealed a slow periodic modulation as a function of trial number. Despite an increased level in noise compared with the Two-way condition, and despite saccades now being produced in random directions, the parametric fit captured well the periodic modulation in the adaptation of saccade amplitude. The posterior densities for the three frequency conditions (Fig. 4*D*, *top left*) yielded estimates of 3 ± 0.12 cpb, 4 ± 0.10 cpb, and 6 ± 0.68 cpb, for the 3, 4, and 6 cpb frequency conditions, respectively. The corresponding estimated amplitudes of the adaptation gain (Fig. 4*D*, *top center*) were 0.14 ± 0.03, 0.17 ± 0.03, and 0.08 ± 0.03 of the ISS amplitude, that is, the adaptation gain reached $14 \pm 3\%$, $17 \pm 3\%$, and $8 \pm 3\%$ of the amplitude of the inducing disturbance. Adaptation gain lagged the ISS by an estimated 14.3 ± 6.5, 22.2 ± 4.1, and 18.5 ± 6.1 trials (Fig. 4*D*, *top right*). Finally, estimates of the drift parameters for the frequency of 3, 4, and 6 cpb, respectively, were -0.46 ± 0.11, -0.43 ± 0.12, and -0.46 ± 0.06 for B_o; 0.19 ± 0.14, 0.15 ± 0.14, and 0.26 ± 0.11 for B; and $9e^{-03} \pm 10e^{-03}$, $16e^{-03} \pm 10e^{-03}$, and $14e^{-03} \pm 9e^{-03}$ trials^{-1} for α (Fig. 4*D*, *bottom*).

Validation of Parameter Estimation Procedure

We validated the presence of distinct periodicity in the data by computing the fast Fourier transform (FFT) of the adaptation gain for each observer and condition. The presence of the peak in the FFT of the variable (Fig. 5, *A* and *B*, show example
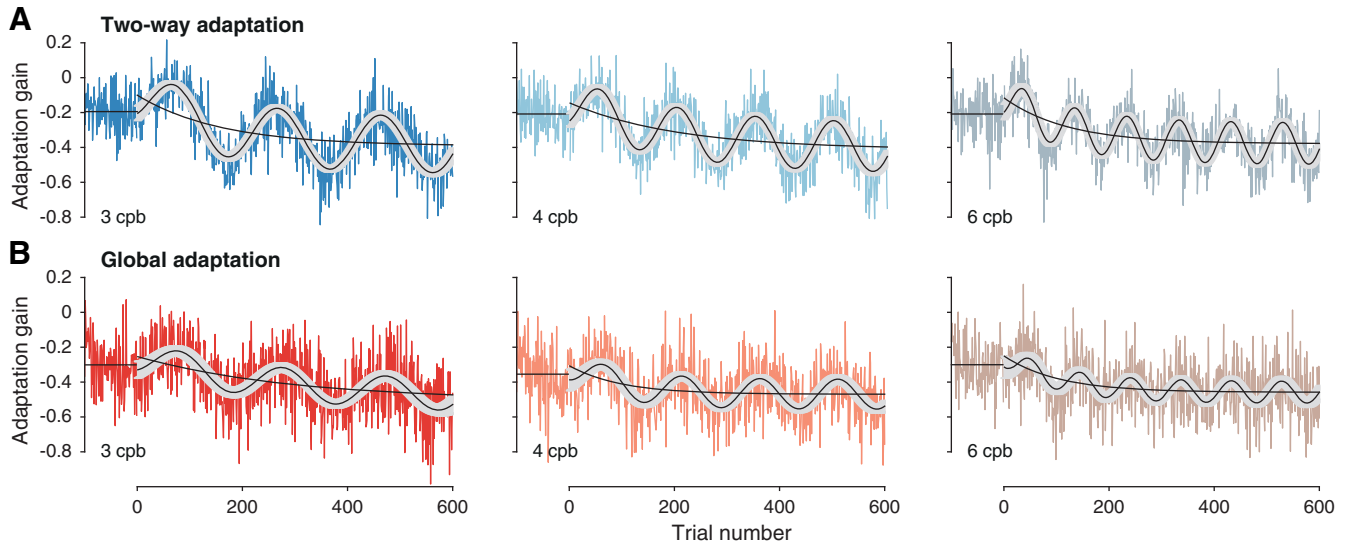
Fig. 3. Average adaptation gain for each frequency in the Two-way (*A*) and Global (*B*) adaptation conditions. Continuous curves depict fits of model B+D+S of Table 2 to the average across participants of the individually demeaned data in each frequency and adaptation type condition. The mean of the block across participants was then added to overlap the fit with the data. Shaded areas are based on the 95% confidence intervals of the parameter estimates.

observer IW) indicates that the oculomotor response acquired a modulation of frequency similar to that of the ISS. The power spectrum of the data, that is, the FFT of the autocorrelation function of the adaptation gain, also shows weight in the spectral power at that frequency (Fig. 5, *C* and *D*, show example *observer IW*), indicating that the autocorrelation function of the signal had a temporal structure reflecting the modulation on the timescale of the stimulus. With the exception of 6 of 120 adaptation blocks (all from the Global adaptation condition), all posterior distributions resulting from our parameter estimation procedure were unimodal and corre-

sponded well to the values of the peaks in the absolute value of the FFT of the same data (Fig. 5, *E* and *F*). Three runs (1 for the 3 cpb, 2 for the 4 cpb conditions) had modes at the frequencies of the stimulus but also presented much smaller secondary peaks at another of the tested frequencies, possibly suggesting a contamination from a previous block. Data from *participant CC* in the Global adaptation type tested at frequencies 3 and 6 cpb gave posteriors with modes at the boundaries of the prior range (2 cpb and 8 cpb for the 6 cpb and 3 cpb conditions tested), suggesting that the data were corrupted by excessive noise. This participant was also the oldest in the
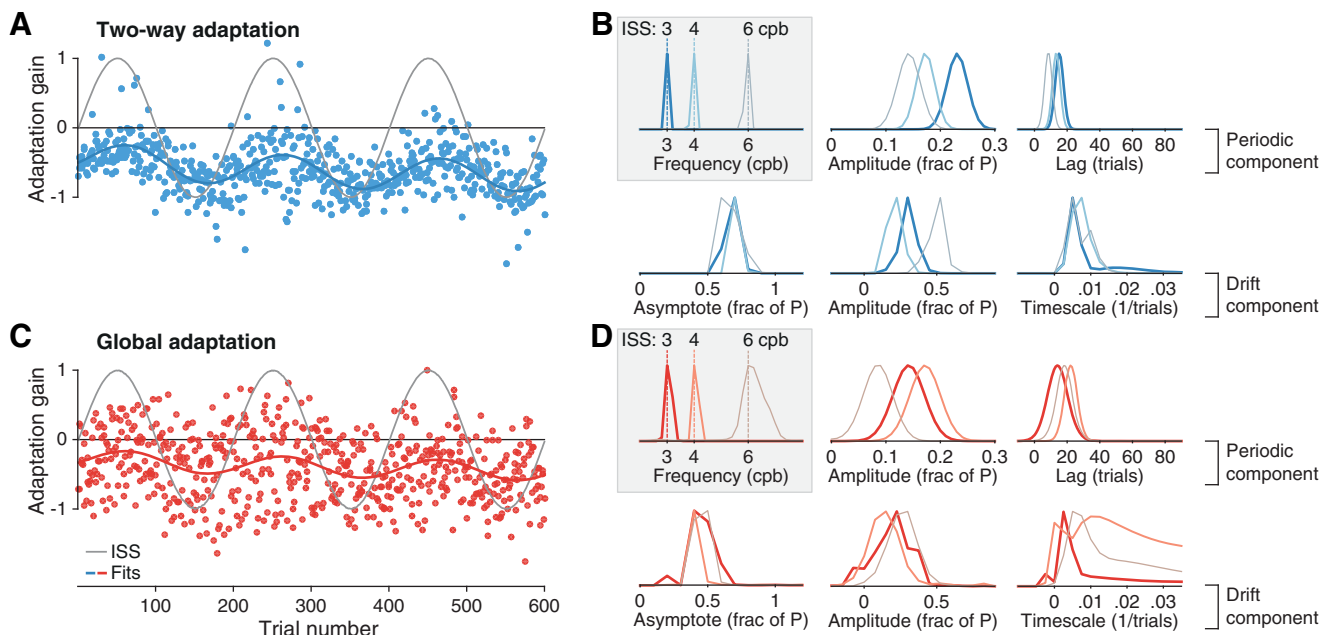

Fig. 4. Example data and parameter estimation from 1 participant (*IW*). *A*: adaptation gain (dots) during Two-way adaptation with a frequency of 3 cpb (200 trials per ISS cycle). Continuous blue line shows the fit to the model with the best-estimated parameters. Thin gray line shows the ISS. *B*: posterior probability densities, normalized to their maximum values, for the frequency, amplitude, and lag parameters of the periodic component of the response (*top*) and for parameters describing the baseline drift (*bottom*) during Two-way adaptation. ISS frequency conditions are color-coded (frequency plot). The modes of the posterior distributions for the frequencies have been selected in a first estimation (gray-shaded panel). The remaining parameters were then estimated at that preferred frequency. *C*: equivalent plot of adaptation gain during Global adaptation. *D*: equivalent posterior probability densities for Global adaptation.
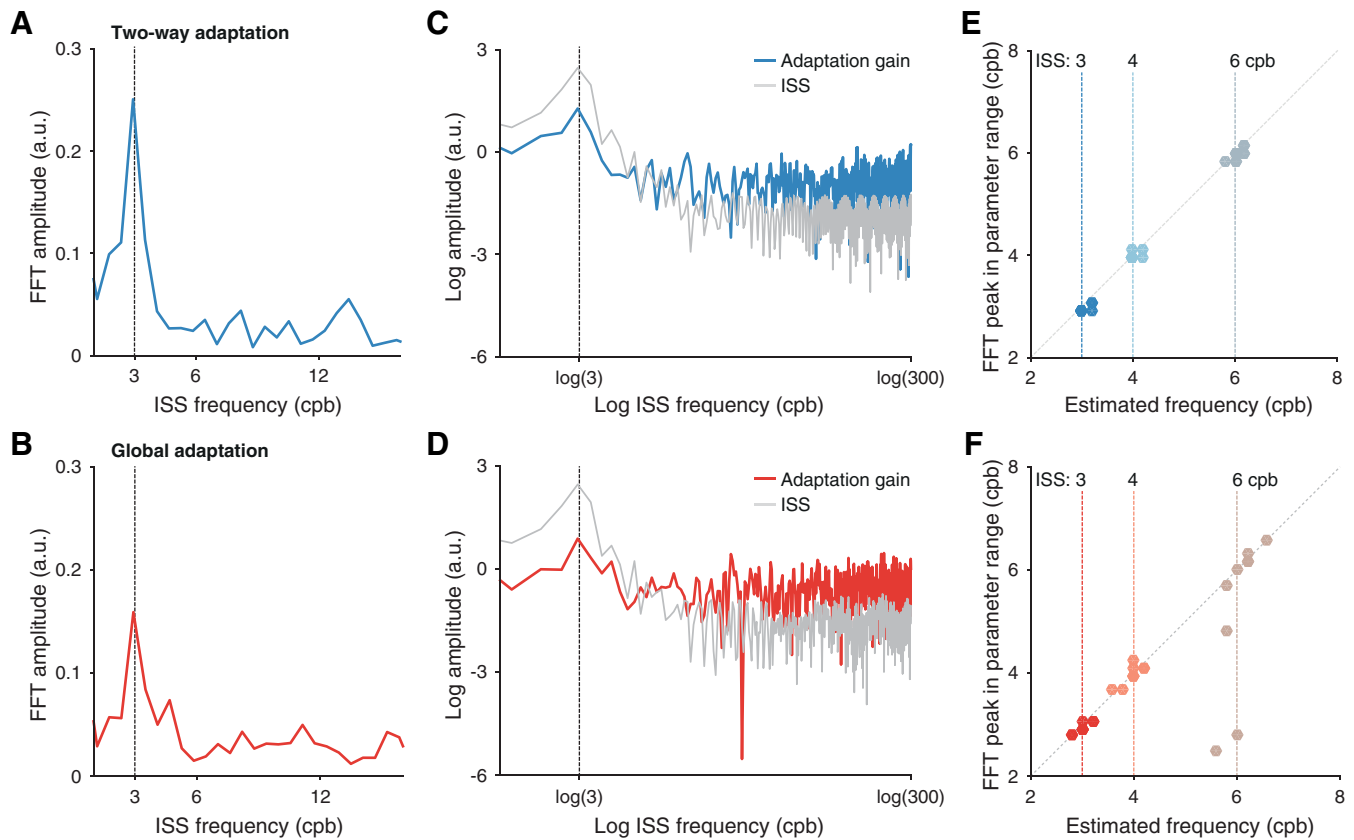
Fig. 5. Validation of the frequency estimation using fast Fourier transform. *A* and *B*: absolute value of the Fourier transform of the adaptation gain for example *observer IW*, for the 3 cpb ISS-frequency condition in Two-way and Global adaptation, respectively. Note the clear peaks at approximately the frequency of the ISS. *C* and *D*: power spectrum of the ISS and the adaptation gain for the same observer. The peak in the power spectrum of the gain at a nonzero frequency (that of the ISS) ensures that its inverse Fourier transform (i.e., the autocorrelation function of the gain) does not display the monotonic decaying pattern that is characteristic in fixed-step adaptation paradigms. *E* and *F*: scatterplots of the estimated frequencies and the peaks of the amplitude of the Fourier transform of the adaptation gain. Note that individual points are superimposed when their estimated frequencies coincided. a.u., Arbitrary units.

group tested, and given that the Global type was clearly more tiring on every participant, it is also possible that this participant's oculomotor system was simply unable to track the sinusoidal disturbance. All Global data for the participant were taken in a single session. Therefore, we excluded all Global adaptation data from this participant from all further analysis. His Two-way adaptation session did not display any obvious anomaly and was retained for full analysis (cf. Fig. 5*E*).

Analysis of Saccadic Response at Population Level

We estimated the model parameters for each of the participants and conditions for both the periodic (Fig. 6, *A–C*, *left*) and drift (Fig. 6, *D–F*, *left*) components of the response. The frequency of the disturbance was consistently extracted across all participants. The data recorded during Global adaptation had much higher variability, but in only 3 (only 1 of which was kept for further analysis) of 30 cases in the Global condition (and none in the Two-way condition) did the frequency estimates differ by >0.5 cpb from the corresponding ISS frequency (Figs. 5*F* and 6*A*; also see below). For Two-way adaptation, the estimated frequencies averaged to 3.06 ± 0.03, 4.04 ± 0.03, and 6.06 ± 0.05 cpb for ISS frequencies of 3, 4, and 6 cpb, respectively (Fig. 6*A*, *right*). In the Global adaptation conditions, the corresponding values were 3.00 ± 0.05, 3.98 ± 0.06, and 6.04 ± 0.10 cpb. The

estimated frequency depended on the ISS frequency $[F(1.47, 11.80) = 1,872.23, P < 0.001]$ but not on adaptation type $[F(1,8) = 1.00, P > 0.250]$ or on the interaction between frequency and adaptation type $[F(1.45, 11.63) = 0.27, P > 0.250]$.

To obtain population averages for parameters other than the frequency, we weighted individual estimates by their reliability (i.e., their SDs). The estimated amplitudes of the adaptation gain in the three Two-way conditions were 0.16 ± 0.01, 0.14 ± 0.01, and 0.12 ± 0.02 or 16%, 14%, and 12% of the amplitude of the ISS (*P*, 2 dva), respectively (Fig. 6*B*, *right*). Correspondingly, for the Global adaptation conditions we estimated gain amplitudes of 0.10 ± 0.01, 0.09 ± 0.01, and 0.08 ± 0.01 or equivalently $10 \pm 1\%$, $9 \pm 1\%$, and $8 \pm 1\%$ of the ISS amplitude. Indeed, amplitudes were significantly higher during Two-way compared with Global adaptation $[F(1,8) = 34.71, P < 0.001]$ and higher for slower modulations than for faster ones $[F(1.30, 10.40) = 10.78, P = 0.005]$. The interaction between ISS frequency and adaptation condition was not significant $[F(1.85, 14.73) = 1.42, P > 0.250]$.

The population estimates for the lags were 20.47 ± 3.85, 16.60 ± 2.27, and 10.49 ± 2.15 trials behind the peak of the ISS for the Two-way adaptation conditions and 28.88 ± 4.48, 24.77 ± 3.40, and 20.49 ± 1.92 trials for the Global adaptation in the 3, 4, and 6 cpb conditions, respectively (Fig. 6*C*, *right*). The ANOVA confirmed that lags were significantly longer in
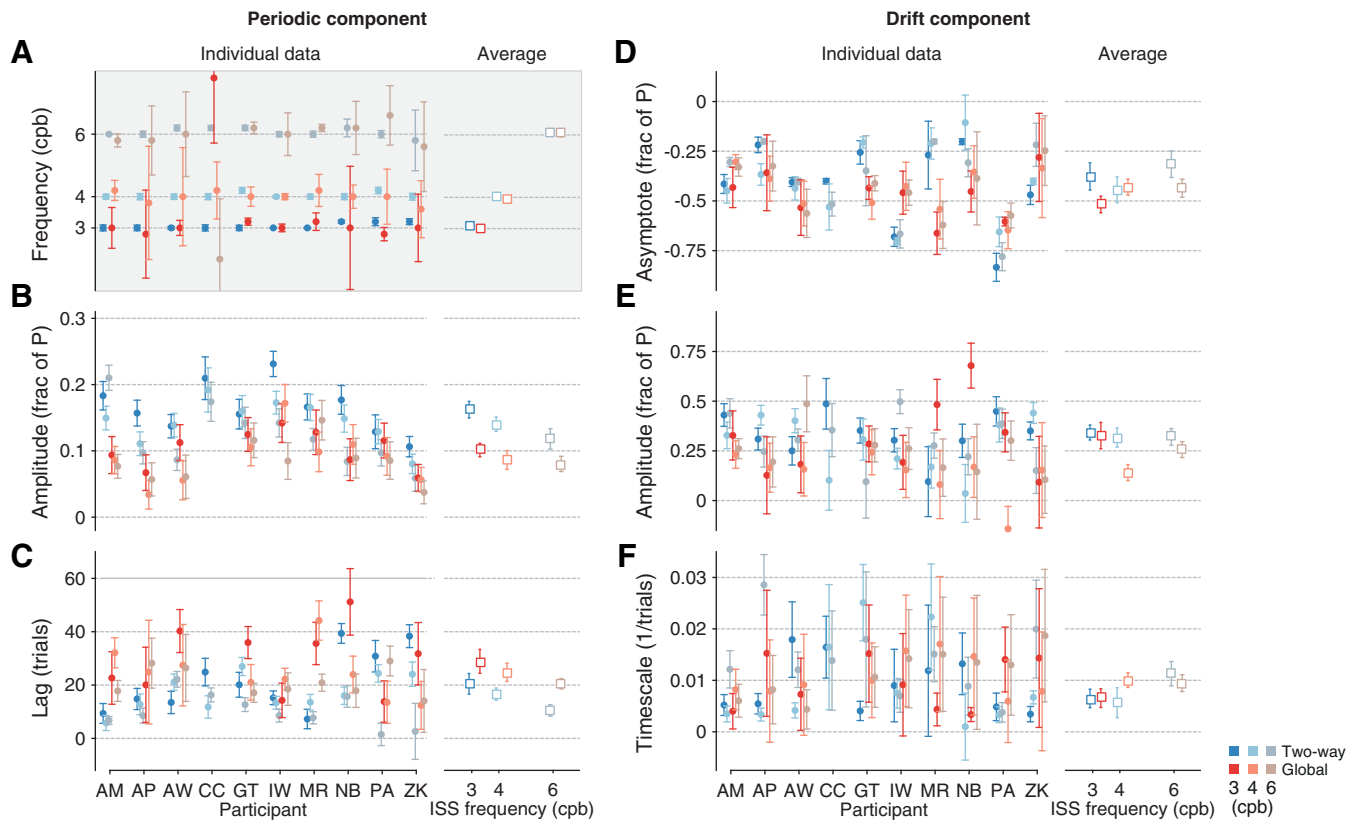
Fig. 6. Parameter estimates as a function of adaptation type and ISS frequency, plotted separately for the 10 participants (*left*; error bars are SDs) and averaged across participants (*right*; error bars are SEs). *A–C*: estimated parameters of the sinusoidal variation of the adaptation gain: frequency in cpb (*A*); amplitude as a proportion of the ISS amplitude *P* (*B*); lag in number of trials trailing the peak of the ISS (*C*). *D–F*: estimated parameters for the drift component of the adaptation gain: baseline asymptote (*D*); amplitude of the drift during the adapting trials (*E*); timescale of the drift (*F*). Gray-shaded panel in *A* highlights that modes of the posterior distributions for the frequencies have been selected in a first estimation. The remaining parameters were then estimated at that preferred frequency. All data have been included in this plot. However, data from *participant CC* in the Global case were removed from further analyses because of unreliable estimation of the frequencies in the 3 cpb and 6 cpb conditions.

the Global than the Two-way adaptation condition [$F(1,8) = 10.66$, $P = 0.011$]. Moreover, lags decreased with ISS frequency [$F(1.31,10.45) = 5.35$, $P = 0.035$], irrespective of adaptation condition [interaction: $F(1.56,12.47) < 1$]. Note, however, that in each condition the cycle has a different length (200, 150, or 100 trials). Therefore, the phase difference between the peaks of the ISS and the adaptation gain (i.e., the relative distance as a portion of the cycle) remains relatively constant (0.67 radians, or ~10% of 1 cycle) in the three Two-way conditions, while it increases somewhat with the frequency (0.91, 1.04, and 1.29 radians, ~15–20% of one cycle) in the Global conditions. An ANOVA on the lag expressed in these units yielded a main effect of adaptation type [$F(1,8) = 17.13$, $P = 0.003$] but no effect of frequency [$F(1.63,13.05) = 0.36$, $P > 0.250$] and no significant interaction between these two factors [$F(1.47,11.77) = 2.02$, $P = 0.165$].

The population estimates for the baseline asymptote B_o (cf. *Eq. 3*; Fig. 6D, *right*) in the Two-way and Global conditions were -0.38 ± 0.07, -0.44 ± 0.06, and -0.32 ± 0.07 and -0.52 ± 0.04, -0.43 ± 0.04, and -0.44 ± 0.05 of the ISS amplitude, respectively. The estimates of the drift amplitude B (cf. *Eq. 3*; Fig. 6E, *right*) gave 0.34 ± 0.04, 0.32 ± 0.05, and 0.32 ± 0.04 of the ISS amplitude in the Two-way conditions and 0.33 ± 0.07, 0.14 ± 0.04, and 0.26 ± 0.04 in the Global conditions. Finally, the decay timescale α (cf. *Eq. 3*; Fig. 6F,

right) was estimated to be $6.5e^{-03} \pm 1.8e^{-03}$, $5.7e^{-03} \pm 2.9e^{-03}$, and $11.3e^{-03} \pm 2.4e^{-03}$ trials^{-1} in each of the Two-way conditions and $6.5e^{-03} \pm 1.8e^{-03}$, $10.0e^{-03} \pm 1.4e^{-03}$, and $9.5e^{-03} \pm 1.6e^{-03}$ trials^{-1} in each of the Global conditions. ANOVAs suggested that these parameters are largely consistent across adaptation types and ISS frequencies, with no significant main effects or interactions on any of the drift parameters (all $F < 3.1$; all $P > 0.11$).

Assessing the Evidence for a Periodic Oculomotor Response

To assess the quality of the fit to the data, we computed the ratio of the odds for the sinusoidal model and the odds for a drift-only model consisting of just the drift in the baseline (Hudson and Landy 2012; Kass and Raftery 1995). The resulting values are called evidence and provided in decibels as 10 times the $\log_{10}$ of the ratio. Positive values of the evidence indicate that the odds of a model that includes the sinusoidal component are higher than those of the drift-only model; we consider evidence exceeding 3 dB as supporting the presence of a sinusoidal signal (Hudson and Landy 2012). We obtained these values for the initial estimation, used to determine the frequency of the response, as well as for the subsequent fixed-frequency estimation, used to estimate all other model parameters. For the initial estimation and Two-way adaptation the values of the evidence ranged from -0.6 to 272 dB, with averages of 108.2 ± 21.3, 88.3 ± 13.7, and 56.9 ± 19.8 dB for

the 3, 4, and 6 cpb conditions, respectively. Apart from a single negative value in a 6 cpb run, the next smallest value was 11.3 dB. Thus for 29 estimates in the Two-way condition we found very strong evidence for the presence of the sinusoidal component compared with a drift-only model. In the initial estimation for the Global conditions, the evidence ranged from −6.7 to 53.4 dB, with averages of 12.7 ± 4.4, 9.8 ± 6.3, and 5.9 ± 4.0 dB for the 3, 4, and 6 cpb conditions, respectively. Seven of 27 evidence values were negative, and an additional 4 had magnitudes < 3 dB.

For the second estimation performed with fixed frequency these numbers improved significantly. For Two-way adaptation in this second stage the values of the evidence ranged between 44 and 669 dB, with averages of 219.0 ± 42.8, 218.3 ± 55.8, and 165.9 ± 32.0 dB for the 3, 4, and 6 cpb conditions, respectively. In the Global conditions, the fixed-frequency estimation yielded evidences ranging between 16.8 and 494.4 dB, with averages of 96.7 ± 22.8, 154.7 ± 50.3, and 92.9 ± 28.8 dB for the 3, 4, and 6 cpb conditions. In this estimation stage, the overall minimum for the evidence was more than fivefold the threshold that would suggest strong support for the sinusoidal model. Therefore, these figures suggest very solid support in favor of the presence of the hypothesized periodic modulation in the oculomotor response.

DISCUSSION

We investigated the oculomotor response to a visual disturbance created by an ISS of the saccade target along the movement direction, which continuously varied across trials following a sinusoidal function. We observed a discernible and reproducible change in saccade amplitude with structural features related to the disturbance. To establish and understand the relation between the visual disturbance and this oculomotor response, our analyses consisted of a three-step approach. First, we fitted a set of formal models to the average of the demeaned individual data. Using statistical model comparison, we found that two additive contributions best described the saccadic response: a sinusoidal modulation of the saccade amplitude (and, consequently, of the adaptation gain) and an exponential drift in the baseline. Second, we used a hierarchical Bayesian parameter estimation procedure to determine the features of this response on an individual basis and compared them across three frequencies of the ISS and two types of adaptation (Two-way and Global; Rolfs et al. 2010). Third, we showed that the individual data strongly support the additive model (sinusoid + drift) as compared to a model assuming the baseline drift alone.

The periodic component of the oculomotor response closely followed the frequency of the ISS across all conditions (no observer's data showed deviations > 10%). Its amplitude was modest (8–16% of the amplitude of the ISS) and larger for Two-way than for Global adaptation and for lower ISS frequencies than for higher ones. At the same time, the oculomotor response lagged the ISS by a constant fraction of the cycle for the three different ISS frequencies and by fewer trials (or a smaller fraction of the cycle) in the Two-way than the Global adaptation condition. In addition to this periodic component of the oculomotor response, we observed substantial drift that increased saccadic undershooting across consecutive trials. This drift was comparable across the three ISS frequencies and

the two types of adaptation (on average 39% of the ISS amplitude in the Two-way adaptation and 44% in the Global conditions). Both contributions should be considered when assessing the degree of efficiency or completeness of adaptation.

Indeed, these results highlight unique features of our empirical approach. In contrast to more traditional saccadic adaptation protocols (see Hopp and Fuchs 2004 for review), our protocol does not require several instantiations per participant to enhance signal-to-noise ratio of the response: we obtained clean parametric fits for individual data sets in almost all cases. Second, our protocol enables dissociation of two consequences of adaptation: an active response to the part of the stimulus that varies systematically across trials (here, a periodic response) and a drift toward larger hypometria that does not vary across stimulus conditions. Many saccadic adaptation protocols find exponential changes in saccade amplitude that may contain such drift superimposed on (and indistinguishable from) the systematic response of the oculomotor system to the altered feedback it receives during adaptation. Finally, the lag of the oculomotor response appears to be an intrinsic feature of sinusoidal adaptation. In fixed-step protocols, the decay timescale τ measures the rate of change of the VE because its size at $n + 1$ has decreased by $1/\tau$ with respect to trial n. For a sinusoidal ISS, the rate of change is provided by its angular frequency, or the change in the phase produced by one trial, $2\pi 1 f / N$. Whereas there may be a lag in fixed-step protocols (e.g., Vaswani and Shadmehr 2013), typical fits of decaying exponentials do not feature a parameter equivalent to the lag, and if they did (e.g., in terms of a delayed exponential), that parameter (and its potential trade-offs with the timescale τ) might not be well constrained by intrinsically noisy saccade gain data.

Relation to Previous Work: Role of Variation and Variability of Experienced Error

The vast bulk of studies on saccadic adaptation have used target displacements of constant size (fixed-step protocols), which generally come in one of two variants. In the first and most common variant, the size of the ISS is a constant proportion of the presaccadic target amplitude (e.g., Herman et al. 2013; Hopp and Fuchs 2004; McLaughlin 1967). In this paradigm, as the amplitude of the saccade adapts, the VE progressively decreases (Fig. 1A). In a second variant (Robinson et al. 2003), the target is also displaced by a constant proportion of the first target step, but relative to the saccade landing position detected right before saccade landing. This manipulation ensures a feedback with constant VE but means that the resulting (surreptitious) extra displacement of the target progressively changes as a proportion of the presaccadic target amplitude (Fig. 1B).

The latter paradigm proved more efficient in inducing adaptation (Robinson et al. 2003), a feature that was argued to be a consequence of the saccadic system experiencing consistently larger VE than a fixed-ISS protocol would have caused. However, others have argued that the oculomotor system predicts—with commendable precision—where to expect the target upon landing (Collins et al. 2009). In this scenario, the ISS is a proxy for the prediction error that, in addition to the VE, can drive adaptation (Collins and Wallman 2012). Because both variants

of these fixed-step protocols (ISS or VE) result in an evolution of the SG, one could argue that the apparently constant disturbances result in passive (or induced) variation in the feedback. With a constant ISS, the variation manifests in the VE; with a constant VE, the variation manifests in the prediction error. The oculomotor system may take this continuous variation as evidence that the error must be attributed to an inaccuracy of the eye's own movement, and not simply to motion of the target in the world, thus inducing saccadic adaptation (see also Wei and Körding 2009).

Other studies have gone beyond the fixed-step protocol by adding random ISS sequences across the adapting trials (Srimal et al. 2008) or by adding variability to the VE while still keeping its mean constant (Havermann and Lappe 2010). Srimal et al. (2008) fitted the trial-by-trial correction to the saccade amplitudes with a delta rule-based state equation, in which adaptation is driven by the difference between the predicted saccade gain and the perturbation experienced on the current trial, weighted by a learning rate. They found that the magnitude of the learning rate was comparable for a fixed ISS and for ISSs that randomly changed between two magnitudes and signs across trials. On the basis of this result, the authors argued for a simple, obligatory learning process underlying saccadic adaptation, in which the oculomotor response is a superposition of trial-by-trial corrections. Havermann and Lappe (2010) used the fixed-VE protocol (Robinson et al. 2003) but added variability to the VE size that was drawn from Gaussian distributions with three different degrees of variability (i.e., standard deviations). The authors reported a marked effect of variability on the adaptation rate that could not be explained by a linear superposition of corrections to the trial-by-trial magnitudes of the VE (when its mean value was kept constant), contrary to what Srimal et al. (2008) proposed.

Indeed, our results suggest that the oculomotor system very clearly differentiates between structured variation of the position of the target and variability in its location. Havermann and Lappe (2010) still observed adaptation when the variability in the VE was larger than the size of the mean. In that condition, however, the efficiency of adaptation was greatly hampered compared with low-variability conditions, suggesting that the system's estimate of the stimulus mean was compromised. Our stimulus had overall zero mean in each adapting block (we used an integer number of cycles). It did not have zero variability, however, even when the size of the second step did not have added jitter. In fact, a sine wave has a variance that increases monotonically to one-half of the square of the amplitude and then remains within a narrow range from this asymptote after the first cycle. Thus our stimulus could be viewed by the oculomotor system as a disturbance that carries a variance of half the square of the ISS amplitude around a mean close to zero beyond the first cycle. If the saccade amplitude on a given trial were based on the statistics of a long trial history (e.g., the entire adaptation block), the change in the mean and variability—throughout the first cycle of the ISS and beyond—would be expected to produce decay in the efficiency of adaptation. This decay should result in a significant reduction of the amplitude of the sinusoidal component, in incomplete cycles, or in erratic frequency. None of these predictions was supported by our data. Instead, we observed a clear periodic variation that can be fitted with an undistorted sinusoid with reduced amplitude, suggesting that the system integrates some share of the recently experienced stimulus rather than the entire stimulus history (see also below).

Possible Origins of Drift

In our data, the clear periodic oculomotor response rode on substantial drift in the baseline saccade gain, increasing hypometria over a block of trials. Its pervasiveness across experimental conditions suggests that this drift is largely stimulus independent. However, it is unlikely to reflect systematic measurement error such as a decrease in calibration accuracy, which would be reflected in biases in the saccadic landing site (*x* and *y* coordinates), not in a continuous reduction of saccade gain.

An alternative explanation of the drift is that our protocol featured both inward (negative ISS) and outward (positive ISS) adaptation, and the latter has been shown to be slower and less efficient in fixed-step protocols (Ethier et al. 2008b; Fuchs et al. 1996; Miller et al. 1981; Robinson et al. 2003; Scudder et al. 1998; Straube et al. 1997). The sinusoidal excursion of the ISS was always symmetrical with respect to the eccentricity of the presaccadic target in both size and trial intervals. The VE also displayed a clear sinusoidal variation (data not shown), which in most of the participants had a positive mean, because SAs were largely hypometric. This hypometria would introduce an effective contribution to the visual feedback of sign opposite to that of the drift observed. Indeed, our cycle lengths were between 100 (6 cpb condition) and 200 (3 cpb condition) trials, with at least 50 positive ISSs followed by 50 negative ISSs, etc. Even assuming hypometria, stronger inward adaptation should leave traces of the reversals of adaptation (e.g., reduced amplitude when the gain increases) or at least slowing down of the trial-by-trial evolution of the drift. None of these effects was apparent in our data. On the contrary, despite the fact that our stimulus introduced an initial imbalance in the outward direction (the first half-period of the ISS was outward), the periodic response followed rapidly with a lag of 10–30 trials on average and we observed the largest increases in hypometria in the beginning of each adaptation block (the drift was well fit by a decaying exponential). Therefore, we do not believe that the pervasive inward drift of the baseline can be explained by inward adaptation being more efficient than outward adaptation.

Yet there was no driving stimulus to explain this drift in the way a constant displacement drives adaptation in fixed-step protocols. Instead, it could be a consequence of the accumulation of some oculomotor bias (Cameron et al. 2015), possibly to minimize saccadic flight time (Harris 1995; Harris and Wolpert 2006)—a requirement that may be exacerbated by the fast pacing used in our experiments (see also Gray et al. 2014)—or a misalignment of proprioception and the visual estimation of target and eye position (Smeets et al. 2006). Alternatively, it may be indicating the presence of a learner with a forgetting rate below unity (Ethier et al. 2008a; Huang and Shadmehr 2009; Smith et al. 2006; van der Kooij et al. 2015). It is worth pointing out that this process should not be understood as a second learning process, unfolding its effect on a different timescale (e.g., Ethier et al. 2008a; Körding et al. 2007; Smith et al. 2006). To address the number of learners involved in adapting to continuously varying stimuli, future studies could combine the present paradigm with error-clamp

trials (cf. Ethier et al. 2008a, 2008b; Smith et al. 2006) or combine multiple frequencies in the same block of adapting trials (see Hudson and Landy 2016 for a related approach).

A (Delta-Rule) State Equation for Sinusoidal Adaptation Data?

Assuming the simplest version of a delta-rule state equation (Nassar et al. 2010; Rescorla and Wagner 1972; Sutton and Barto 1981), Srimal et al. (2008) demonstrated that, in saccadic adaptation, learning takes place even when visual feedback cannot be used to improve overall behavior, via a mechanism that is rapid and obligatory and does not require conscious awareness. They based this conclusion on the fact that they could fit saccadic adaptation data in two different paradigms—a fully consistent and a pseudorandom stimulus—using a single learning rate of comparable magnitude. This conclusion seems to leave little space for involvement of more than the last experienced feedback in the error-correction mechanism. While this may be true, it is puzzling how humans could track correlated stimulus sequences if their sensorimotor system only relies on its latest observed value (Baddeley et al. 2003; Burge et al. 2008) or show oculomotor adjustments dependent on errors correlated over long timescales (Wong and Shelhamer 2011b, 2014). Inspection of the mathematical consequences of the iteration implied in their state equation (e.g., Cheng and Sabes 2006) shows that any part of the postsaccadic target amplitude that is held constant across a set of adaptation trials will result in an asymptotic bound for the saccade amplitude. If the ISS is changed randomly, with no correlation from one trial to the next, the state equation predicts a wandering evolution of the size of the saccade amplitude in between the asymptotes set by both sizes of the ISS used, in agreement with what the authors observed (Srimal et al. 2008).

However, when a similar algorithm is applied to a correlated stimulus (e.g., a random walker or a sinusoidal disturbance), the same state equation predicts an extra term that has the form of a convolution of the ISS with weights given by powers of a function of the learning rate. Because of the weights being powers of a number smaller than unity, there will be an effective number of trials beyond which adding the effect of more trials will not make much difference. This term could be seen as defining a response function of the saccadic system that convolves the (variable part of the) disturbance. The presence of a lag in the response underscores such integration. Viewed from this perspective, an error-correcting mechanism that changes the adaptive state of the oculomotor system—via the delta rule algorithm—may have developed to extract correlations present in the disturbance that may need to be tracked to mitigate its effect. In agreement with this idea, studies of visuomotor adaptation in manual reaching have found stronger or more persistent adaptation for highly correlated stimuli (Castro et al. 2014; Huang and Shadmehr 2009) and saccadic adaptation shows higher completeness with gradually changing stimuli (Wong and Shelhamer 2011a) or when the disturbances involve very small ISSs (Herman et al. 2013).

In summary, the idea that only the last experienced feedback matters (Collins 2014; Srimal et al. 2008) may be true, but the widespread use of disturbances with very limited internal dynamics may have undermined the ability of the system to track the stimulus and extract its correlation content. The return-to-baseline adaptation observed in fixed-step protocols would then result as a consequence of the specific dynamics of those disturbances. Thus using disturbances with more varied dynamics may help constrain delta-rule state equation models of adaptive human responses and extract realistic parameters for the learning rates. We defer a quantitative analysis of this point of view to a further communication.

Higher Environmental Consistency Improves Adaptation Rate

Motor adaptation occurs through the continual recalibration (or updating) of a sensorimotor mapping. The feedback error that drives this recalibration can have random (i.e., observation, measurement, or execution noise) or systematic (i.e., correlation between successive instances of the feedback) components. It has been argued that the learning rate would be hampered by higher random noise while a higher component of the systematic part would enhance it. In the case of a random walker, a higher drift of the walker has been associated with driving higher such recalibration (Burge et al. 2008).

Because a sinusoidal ISS clearly displays a consistent correlation in the size of the steps that the disturbance takes across trials, our stimulus indeed resembles a walker with a systematic displacement across trials, as opposed to being random. In our data, the drift of the walker would be associated with a trial-by-trial rate of change in the disturbance—its angular frequency or the change of phase produced by one trial. Such rate will grow proportional to the frequency of the disturbance. On that basis one would expect the learning rate to grow higher as the frequency increases. In fact, our data suggest the opposite: we obtained most efficient adaptation at the lowest frequency tested.

This result may become more intuitive when we consider an alternative view of "consistency"—one not strictly associated to the variability in the stimulus (Havermann and Lappe 2010) but to its degree of correlation (Castro et al. 2014; Huang and Shadmehr 2009). A highly correlated stimulus would change little from one trial to the next, providing confidence to the sensorimotor system to learn the stimulus more efficiently. Castro and collaborators (2014) have suggested an operational definition of stimulus consistency based on its lag-1 autocorrelation function. In the case of a sinusoidal disturbance that is precisely the cosine of its angular frequency (note that for a larger frequency the cosine of the angular frequency and consequently the lag-1 autocorrelation of the stimulus will be smaller). Furthermore, these authors argued that a higher value of this property in the stimulus would result in higher adaptation. This prediction is consistent with what we observe in our data on average and in each individual data set, which may point to a difference in learning rates between ISS frequency conditions.

Differences Between Vector-Specific and Global Adaptation and Potential Neural Substrates

Recent studies have challenged the notion that saccadic adaptation is genuinely vector specific—previously considered a hallmark of oculomotor learning (Hopp and Fuchs 2004)—and suggested instead that adaptation of a large range of saccade amplitudes and directions can develop rapidly at the same time (Garaas and Pomplun 2011; Rolfs et al. 2010). Our

Global and Two-way adaptation conditions (adopted from Rolfs et al. 2010) allow us to venture a comparison of the dynamics of global and vector-specific adaptation. Adaptation in the Global condition reached a lower degree of completeness than in the Two-way condition, with lags about twice as long. At least three different explanations may account for these differences.

The first (and the least exciting) explanation is a difference in observers' awareness of the induced target steps. Recently, Collins (2014) suggested that awareness of the target step may lead to less efficient adaptation, perhaps as a result of an attribution of the target step to external motion rather than insufficiency of the movement program (Robinson et al. 2003; Wei and Körding 2009). To explain our findings in this light, however, the ISS would need to be more readily detected for saccades in random than in horizontal directions, a prediction that is at odds with the subjective reports of our observers and that finds little support in published data (Bansal et al. 2015; Rolfs et al. 2010).

A second explanation of a reduced amplitude and increased lag of the periodic oculomotor response in the Global condition is that global adaptation is in fact just the result of a superposition of vector-specific adaptation of each saccade vector (with some transfer to similar saccade vectors). As a consequence, adaptation would progress more slowly if many saccade directions were adapted at the same time. On the basis of simulations of the evolution of global saccade gain in this scenario, Rolfs et al. (2010) have ruled out this explanation for their data: A continuous summation of vector-specific adaptation in many directions fell short of the completeness of adaptation observed in the Global condition. The authors only tested inward adaptation in the fixed-step protocol, in which—as we pointed out above—the observed adaptation may be contaminated with additive drift toward stronger hypometria. However, our present results suggest that this drift is of similar magnitude and time course in the Global and Two-way conditions, such that the authors' argument still holds. Therefore, the present data constitute the first recordings of global adaptation with ISS other than fixed and inward, showing consistent and significant adaptation of the SA, irrespective of the random directions of the saccades conforming to the ISS cycle.

Perhaps the most likely (and certainly the most intriguing) explanation of the differences in lag and amplitude is that during Global saccadic adaptation the system uses an integration window that reaches further into the past, giving less weight to any single ISS experienced. Indeed, reducing the "consistency" weights may be a reasonable strategy of the system when the direction of the saccade is changing randomly and the error signals contain more intrinsic variability (landing sites, and thus VEs, were more variable in Global than in Two-way adaptation). This strategy would indeed predict a reduced magnitude and more delayed response of the oculomotor system without implying a less efficient learning process.

These differences must be reflected in the neural processes underlying learning in the oculomotor system. Indeed, the emerging picture of the neurophysiological processes giving rise to adaptation of targeting saccades involves the coordination of a number of brain structures. In brief, the superior colliculus (SC), a retinotopically organized midbrain structure, may generate an error signal, resulting in vector-specific adaptation of SG (Kaku et al. 2009; Soetedjo et al. 2009). The oculomotor portion of the cerebellum may then use this signal to yield fine adjustments in saccade gain. Evidence from anatomical, electrophysiological, inactivation, and lesion studies suggests that the oculomotor vermis (OV) is a crucial part of the adaptation pathway downstream of the SC (see Dash and Thier 2014 for review). In particular, the duration of bursts in the OV shows a gradual change that is commensurate with the gradual changes in amplitude seen in the fixed-step paradigm (Catz et al. 2008; Kojima et al. 2010). The cerebellum's caudal fastigial nucleus, which shows a similar discharge pattern (Inaba et al. 2003; Scudder and McGee 2003), is thought to inherit this discharge pattern from the OV, to then relay it to the saccadic burst generator in the brain stem (Kojima et al. 2008), resulting in the adapted saccade amplitude.

Whereas these physiological results provide a consistent account of vector-specific adaptation, a learning signal yielding global saccadic adaptation has yet to be found. This learning signal may well have a different origin than the SC and may thus yield different learning coefficients implemented downstream. Indeed, neurons in the OV can be selective or unselective for saccade direction (Kase et al. 1980), suggesting largely different innervation. Alternatively, cerebellar target regions downstream of the SC (including the OV and the fastigial nucleus) may track the spatial statistics of the learning signals they receive and form vector specificity only if signals originate from the same site in the SC over many saccades. Indeed, in this scenario, global adaptation would be the default response of the system to experienced error signals. Vector-specific adaptation, in turn, would be a consequence of increasing selectivity of a spatial prior, perhaps by altering the efficacy of the relevant subsets of direction-selective neurons (Schweighofer et al. 1996a, 1996b). By allowing us to closely track the time dependence of SG and corresponding neural signals at the same time, our paradigm has great promise to elucidate differences in the neural underpinnings between vector-specific and global adaptation.

Conclusions

Using a continuous and periodic disturbance, sinusoidal adaptation provides a novel and effective way to test the plasticity of saccadic behavior. In combination with a sensitive parameter estimation procedure we uncovered the global average response of the system to such disturbance. The paradigm comes with a number of experimental advantages with respect to the traditional fixed-step protocol, including intrinsic features that tap the temporal properties of adaptation in the oculomotor system in an unprecedented way. Adopting this paradigm in this field promises to fundamentally improve our understanding of the dynamics of oculomotor plasticity in healthy participants and to probe its alterations in clinical populations.

DISCLOSURES

No conflicts of interest, financial or otherwise, are declared by the author(s).

AUTHOR CONTRIBUTIONS

C.R.C., S.O., and M.R. conception and design of research; C.R.C. performed experiments; C.R.C. analyzed data; C.R.C., S.O., and M.R. interpreted results of experiments; C.R.C. and M.R. prepared figures; C.R.C. and M.R. drafted manuscript; C.R.C., S.O., and M.R. edited and revised manuscript; C.R.C., S.O., and M.R. approved final version of manuscript.

REFERENCES

Akaike H. A new look at the statistical model identification. *IEEE Trans Automat Contr* 19: 716–723, 1974.

Akaike H. A new look at the Bayes procedure. *Biometrika* 65: 53–59, 1978.

Alahyane N, Devauchelle AD, Salemme R. Spatial transfer of adaptation of scanning voluntary saccades in humans. *Neuroreport* 19: 37–41, 2008a.

Alahyane N, Fonteille V, Urquizar C, Salemme R, Nighoghossian N, Pelisson D, Tilikete C. Separate neural substrates in the human cerebellum for sensory-motor adaptation of reactive and of scanning voluntary saccades. *Cerebellum* 7: 595–601, 2008b.

Albano JE. Adaptive changes in saccade amplitude: oculocentric or orbito-centric mapping? *Vision Res* 36: 2087–2098, 1996.

Azadi R, Harwood MR. Visual cues that are effective for contextual saccade adaptation. *J Neurophysiol* 111: 2307–2319, 2014.

Baddeley RJ, Ingram HA, Miall RC. System identification applied to a visuomotor task: near-optimal human performance in a noisy changing task. *J Neurosci* 23: 3066–3075, 2003.

Bansal S, Jayet Bray LC, Peterson MS, Joiner WM. The effect of saccade metrics on the corollary discharge contribution to perceived eye location. *J Neurophysiol* 113: 3312–3322, 2015.

Bock O, Ilieva M, Grigorova V. Effects of old age and resource demand on double-step adaptation of saccadic eye movements. *Exp Brain Res* 232: 2821–2826, 2014.

Bozdogan H. Model selection and Akaike's Information Criterion (AIC): The general theory and its analytical extensions. *Psychometrika* 52: 345–370, 1987.

Brainard DH. The psychophysics toolbox. *Spat Vis* 10: 433–436, 1997.

Bretthorst GL. *Bayesian Spectrum Analysis and Parameter Estimation.* Berlin: Springer, 1988.

Bridgeman B, Hendry D, Stark L. Failure to detect displacement of the visual world during saccadic eye movements. *Vision Res* 15: 719–722, 1975.

Burge J, Ernst MO, Banks MS. The statistical determinants of adaptation rate in human reaching. *J Vis* 8: 20.1–20.19, 2008.

Cameron BD, de la Malla C, López-Moliner J. Why do movements drift in the dark? Passive versus active mechanisms of error accumulation. *J Neurophysiol* 114: 390–399, 2015.

Castro LN, Hadjiosif AM, Hemphill MA, Smith MA. Environmental consistency determines the rate of motor adaptation. *Curr Biol* 24: 1050–1061, 2014.

Catz N, Dicke PW, Thier P. Cerebellar-dependent motor learning is based on pruning a Purkinje cell population response. *Proc Natl Acad Sci USA* 105: 7309–7314, 2008.

Chen-Harris H, Joiner WM, Ethier V, Zee DS, Shadmehr R. Adaptive control of saccades via internal feedback. *J Neurosci* 28: 2804–2813, 2008.

Cheng S, Sabes PN. Modeling sensorimotor learning with linear dynamical systems. *Neural Comput* 18: 760–793, 2006.

Collins T. Trade-off between spatiotopy and saccadic plasticity. *J Vis* 14: 28, 2014.

Collins T, Heed T, Röder B. Visual target selection and motor planning define attentional enhancement at perceptual processing stages. *Front Hum Neurosci* 4: 14, 2010.

Collins T, Rolfs M, Deubel H, Cavanagh P. Post-saccadic location judgments reveal remapping of saccade targets to non-foveal locations. *J Vis* 9: 29.1–29.9, 2009.

Collins T, Wallman J. The relative importance of retinal error and prediction in saccadic adaptation. *J Neurophysiol* 107: 3342–3348, 2012.

Cornelissen FW, Peters EM, Palmer J. The Eyelink Toolbox: eye tracking with MATLAB and the Psychophysics Toolbox. *Behav Res Methods Instrum Comput* 34: 613–617, 2002.

Dash S, Thier P. Cerebellum-dependent motor learning: lessons from adaptation of eye movements in primates. *Prog Brain Res* 210: 121–155, 2014.

Engbert R, Mergenthaler K. Microsaccades are triggered by low retinal image slip. *Proc Natl Acad Sci USA* 103: 7192–7197, 2006.

Ethier V, Zee DS, Shadmehr R. Spontaneous recovery of motor memory during saccade adaptation. *J Neurophysiol* 99: 2577–2583, 2008a.

Ethier V, Zee DS, Shadmehr R. Changes in control of saccades during gain adaptation. *J Neurosci* 28: 13929–13937, 2008b.

Fuchs AF, Reiner D, Pong M. Transfer of gain changes from targeting to other types of saccade in the monkey: constraints on possible sites of saccadic gain adaptation. *J Neurophysiol* 76: 2522–2535, 1996.

Garaas TW, Pomplun M. Distorted object perception following whole-field adaptation of saccadic eye movements. *J Vis* 11: 2, 2011.

Golla H, Tziridis K, Haarmeier T, Catz N, Barash S, Thier P. Reduced saccadic resilience and impaired saccadic adaptation due to cerebellar disease. *Eur J Neurosci* 27: 132–144, 2007.

Gray MJ, Blangero A, Herman JP, Wallman J, Harwood MR. Adaptation of naturally paced saccades. *J Neurophysiol* 111: 2343–2354, 2014.

Harris CM. Does saccadic undershoot minimize saccadic flight-time? A Monte-Carlo study. *Vision Res* 35: 691–701, 1995.

Harris CM, Wolpert DM. The main sequence of saccades optimizes speed-accuracy trade-off. *Biol Cybern* 95: 21–29, 2006.

Harwood MR, Wallman J. Temporal dynamics and strategy in saccade adaptation (Abstract). *Neuroscience Meeting Planner* 2004: 990.21–11, 2004.

Havermann K, Lappe M. The influence of the consistency of postsaccadic visual errors on saccadic adaptation. *J Neurophysiol* 103: 3302–3310, 2010.

Herman JP, Cloud CP, Wallman J. End-point variability is not noise in saccade adaptation. *PLoS One* 8: e59731, 2013.

Hopp JJ, Fuchs AF. The characteristics and neuronal substrate of saccadic eye movement plasticity. *Prog Neurobiol* 72: 27–53, 2004.

Huang VS, Shadmehr R. Persistence of motor memories reflects statistics of the learning event. *J Neurophysiol* 102: 931–940, 2009.

Hudson TE, Landy MS. Measuring adaptation with a sinusoidal perturbation function. *J Neurosci Methods* 208: 48–58, 2012.

Hudson TE, Landy MS. Sinusoidal error perturbation reveals multiple coordinate systems for sensorymotor adaptation. *Vision Res* 119: 82–98, 2016.

Inaba N, Iwamoto Y, Yoshida K. Changes in cerebellar fastigial burst activity related to saccadic gain adaptation in the monkey. *Neurosci Res* 46: 359–368, 2003.

Jeffreys H. An invariant form for the prior probability in estimation problems. *Proc R Soc Lond A Math Phys Sci* 186: 453–461, 1946.

Kaku Y, Yoshida K, Iwamoto Y. Learning signals from the superior colliculus for adaptation of saccadic eye movements in the monkey. *J Neurosci* 29: 5266–5275, 2009.

Kase M, Miller DC, Noda H. Discharges of Purkinje cells and mossy fibres in the cerebellar vermis of the monkey during saccadic eye movements and fixation. *J Physiol* 300: 539–555, 1980.

Kass RE, Raftery AE. Bayes factors. *J Am Stat Assoc* 9: 773–795, 1995.

Kleiner M, Brainard DH, Pelli DG, Ingling A, Murray R, Broussard C. What's new in Psychtoolbox-3? *Perception* 36: 1–16, 2007.

Kojima Y, Iwamoto Y, Robinson FR, Noto CT, Yoshida K. Premotor inhibitory neurons carry signals related to saccade adaptation in the monkey. *J Neurophysiol* 99: 220–230, 2008.

Kojima Y, Soetedjo R, Fuchs AF. Changes in simple spike activity of some Purkinje cells in the oculomotor vermis during saccade adaptation are appropriate to participate in motor learning. *J Neurosci* 30: 3715–3727, 2010.

Körding KP, Tenenbaum JB, Shadmehr R. The dynamics of memory as a consequence of optimal adaptation to a changing body. *Nat Neurosci* 10: 779–786, 2007.

MacAskill MR, Anderson TJ, Jones RD. Saccadic adaptation in neurological disorders. *Prog Brain Res* 140: 417–431, 2002.

McLaughlin SC. Parametric adjustment in saccadic eye movements. *Percept Psychophys* 2: 359–362, 1967.

Miller JM, Anstis T, Templeton WB. Saccadic plasticity: parametric adaptive control by retinal feedback. *J Exp Psychol Hum Percept Perform* 7: 356–366, 1981.

Nassar MR, Wilson RC, Heasly B, Gold JI. An approximately Bayesian delta-rule model explains the dynamics of belief updating in a changing environment. *J Neurosci* 30: 12366–12378, 2010.

Ostendorf F, Kilias J, Ploner CJ. Theta-burst stimulation over human frontal cortex distorts perceptual stability across eye movements. *Cereb Cortex* 22: 800–810, 2012.

Ostendorf F, Liebermann D, Ploner CJ. Human thalamus contributes to perceptual stability across eye movements. *Proc Natl Acad Sci USA* 107: 1229–1234, 2010.

Panouillères M, Alahyane N, Urquizar C, Salemme R, Nighoghossian N, Gaymard B, Tilikete C, Pelisson D. Effects of structural and functional cerebellar lesions on sensorimotor adaptation of saccades. *Exp Brain Res* 231: 1–11, 2013.

Pelli DG. The VideoToolbox software for visual psychophysics: transforming numbers into movies. *Spat Vis* 10: 437–442, 1997.

Rescorla RA, Wagner AR. A theory of Pavlovian conditioning: variations in the effectiveness of reinforcement and nonreinforcement. In: *Classical Conditioning II: Current Research and Theory*. New York: Appleton-Century-Crofts, 1972.

Robinson FR, Noto CT, Bevans SE. Effect of visual error size on saccade adaptation in monkey. *J Neurophysiol* 90: 1235–1244, 2003.

Rolfs M, Knapen T, Cavanagh P. Global saccadic adaptation. *Vision Res* 50: 1882–1890, 2010.

Rolfs M, Vitu F. On the limited role of target onset in the gap task: support for the motor-preparation hypothesis. *J Vis* 7: 7.1–7.20, 2007.

Rösler L, Rolfs M, van der Stigchel S, Neggers SF, Cahn W, Kahn RS, Thakkar KN. Failure to use corollary discharge to remap visual target locations is associated with psychotic symptom severity in schizophrenia. *J Neurophysiol* 114: 1129–1136, 2015.

Schwarz G. Estimating the dimension of a model. *Ann Stat* 6: 461–464, 1978.

Schweighofer N, Arbib MA, Dominey PF. A model of the cerebellum in adaptive control of saccadic gain. I. The model and its biological substrate. *Biol Cybern* 75: 19–28, 1996a.

Schweighofer N, Arbib MA, Dominey PF. A model of the cerebellum in adaptive control of saccadic gain. II. Simulation results. *Biol Cybern* 75: 29–36, 1996b.

Scudder CA, Batourina EY, Tunder GS. Comparison of two methods of producing adaptation of saccade size and implications for the site of plasticity. *J Neurophysiol* 79: 704–715, 1998.

Scudder CA, McGee DM. Adaptive modification of saccade size produces correlated changes in the discharges of fastigial nucleus neurons. *J Neurophysiol* 90: 1011–1026, 2003.

Smeets JB, van den Dobbelsteen JJ, de Grave DD, van Beers RJ, Brenner E. Sensory integration does not lead to sensory calibration. *Proc Natl Acad Sci USA* 103: 18781–18786, 2006.

Smith MA, Ghazizadeh A, Shadmehr R. Interacting adaptive processes with different timescales underlie short-term motor learning. *PLoS Biol* 4: 1035–1043, 2006.

Soetedjo R, Fuchs AF, Kojima Y. Subthreshold activation of the superior colliculus drives saccade motor learning. *J Neurosci* 29: 15213–15222, 2009.

Srimal R, Diedrichsen J, Ryklin EB, Curtis CE. Obligatory adaptation of saccade gains. *J Neurophysiol* 99: 1554–1558, 2008.

Straube A, Fuchs AF, Usher S, Robinson FR. Characteristics of saccadic gain adaptation in rhesus macaques. *J Neurophysiol* 77: 874–895, 1997.

Sutton RS, Barto AG. Toward a modern theory of adaptive networks: expectation and prediction. *Psychol Rev* 88: 135–170, 1981.

van der Kooij K, Brenner E, van Beers RJ, Smeets JB. Visuomotor adaptation: how forgetting keeps us conservative. *PLoS One* 10: e0117901, 2015.

Vaswani PA, Shadmehr R. Decay of motor memories in the absence of error. *J Neurosci* 33: 7700–7709, 2013.

Wang Y, Liu Q. Comparison of Akaike information criterion (AIC) and Bayesian information criterion (BIC) in selection of stock-recruitment relationships. *Fish Res* 77: 220–225, 2006.

Wei K, Körding K. Relevance of error: what drives motor adaptation? *J Neurophysiol* 101: 655–664, 2009.

Wei K, Wert D, Körding K. The nervous system uses nonspecific motor learning in response to random perturbations of varying nature. *J Neurophysiol* 104: 3053–3063, 2010.

Wong AL, Shelhamer M. Saccade adaptation improves in response to gradually introduced stimulus perturbation. *Neurosci Lett* 500: 207–211, 2011a.

Wong AL, Shelhamer M. Exploring the fundamental dynamics of error-based motor learning using a stationary predictive-saccade task. *PLoS One* 6: e25225, 2011b.

Wong AL, Shelhamer M. Similarities in error processing establish a link between saccade prediction at baseline and adaptation performance. *J Neurophysiol* 111: 2084–2093, 2014.